On-line Adaptation of Underwater Acoustic Transmission Rates to Optimize Communications for Collaborative AUV Missions

Dainis Nams, *Member* IEEE, Mae L. Seto, *Senior Member* IEEE, John J. Leonard, *Fellow* IEEE

***Abstract*— A framework for on-line characterization of, and intelligent adaptation to, changing communication environment conditions is implemented on autonomous underwater vehicles (AUVs). Adopted by the authors to optimize use of the communications channel during collaborative shallow water AUV missions, this framework has application to a variety of on-line communications environment estimation scenarios within the robotics community. A software database tracks the success of data transmitted between multiple agents, providing communications layer visibility into current channel conditions. In the author's AUV implementation, a rate selector chooses optimal transmission rates given current conditions. Outcomes are improvements in bandwidth, reduction in modem power draw, and increased visibility into data success compared to traditional, constant-rate acoustic communication patterns.**

I. Introduction

Autonomous underwater vehicles (AUV) are widely used in applications such as seabed survey, hull inspection, environmental monitoring, and naval threat detection. Initially used singly, AUVs are increasingly collaborating on large-scale missions. While many collaborative AUV applications exist, naval mine counter-measures missions (NMCM) are of particular interest to Defence R & D Canada (DRDC).

If implemented as a collaborative mission, NMCM requires a robust communications network. Electromagnetic and light waves are quickly attenuated underwater, leaving acoustic modems with the most practical range for inter-AUV communication. However, acoustic communications are limited to low frequency (<50kHz) carrier bands due to frequency-dependent absorption [1]. Network bandwidths are further reduced by scattering, ambient noise sources, and time-varying sound speed profiles. These factors limit typical mean bandwidths to the order of bytes per second (B/s) rather than the kB/s and MB/s available on in-air radio networks. While these low rates are sufficient for status updates they do not facilitate high-bandwidth collaborative algorithms such as distributed Simultaneous Localization And Mapping (SLAM), a research topic for DRDC Atlantic.

A fixed-cycle, fixed data rate Time Division Multiple Access (TDMA) is the most commonly implemented access scheme for survey-type collaborative missions [1]. Modems provide a variety of data rates, allowing operators to trade bandwidth for reliability through transmission rate selection. The WHOI Micromodem used throughout this work has the data rates shown in TABLE I.

TABLE I. WHOI Micromodem Data Rate Comparison [2]

WHOI Micromodem Data Rate	Frame Size (Bytes)	Number of Frames per Packet	Packet Size (Bytes)
FSK Rate 0	32	1	32
PSK Rate 1	64	3	192
PSK Rate 4	256	2	512
PSK Rate 5	256	8	2048

Increased underwater communications bandwidth by intelligently using existing modem technology is an active research area. Schneider presents a simple alternating high and low data rate [3] solution as well as an optimal vehicle path solution [4]. Chen and Pompilli implement an optimal message routing scheme [5]. These efforts proved effective in the scenarios to which they were applied, but they are not general enough to be applied to scenarios such as NMCM due to the constraints it imposes on AUV behaviour. Specifically, the above mentioned algorithms require either the ability to influence the mission path or a sensor suite yielding full knowledge of the surrounding acoustic conditions. An approach is required that can effectively improve communications for any mission, regardless of available sensors, operational depth, or mission plan.

Presented is a framework that uses an on-line adaptive transmission rate selector along with improved data transmission performance tracking. Applied to NMCM, these allow the generic AUV to intelligently adapt its transmission rate by learning from the past rather than relying on unavailable sensor information. The contributions of this paper are as follows:

- Quantitative analysis of the relative performance of four WHOI micromodem transmission rates using data collected from October 2013 field trials.
- Robust and bandwidth-cheap data transmission performance tracking to reduce instances of lost data or duplicate transmissions.
- Transmission rate selector adapts on-line for optimal use of communications channel in dynamic environments.

The remainder of this paper is organized as follows. Section II presents the results of preliminary modem characterization field trials. Section III presents the design of a physics-based acoustic and mission simulation environment while Section IV compares the influence of mission factors on communication performance. Section V presents the data transmission

978-0-933957-43-5 ©2015 Crown

performance tracking and rate selection design followed by concluding remarks in Section VI.

II. MODEM RATE CHARACTERIZATION

To develop communication algorithms that optimally adapt the data rate a modem communicates at, the relative reliability of the data rates must be characterized. While it is understood that lower bandwidth transmissions provide a more robust link than high bandwidth rates [3], there has been little work done to characterize the relative probability of frame success for the WHOI data rates in real conditions. The most comprehensive work performed modem hardware / software simulations to compare frame error rates to SNR [5]. However, only ideal deep-water cases were studied and no field experiment validation was presented. Shallow water field trials are required to characterize the relative performance between data rates in representative NMCM conditions.

Such trials were conducted in Bedford Basin (Halifax, NS, Canada). Communications were implemented between two WHOI micromodems with co-processors installed to allow use of PSK data rates [2]. One micromodem was in a stationary tow fish transducer suspended from the moon pool of the DRDC Acoustic Calibration Barge (ACB). The second micromodem was installed in an IVER2 man portable AUV. MOOS-IVP [6] autonomy tools with the Goby2 acoustic communications package was used to control the modem transmissions. Goby implements the Dynamic Compact Control Language (DCCL) [7] to compress data for transmission over low bandwidth acoustic links. A simple two-way communications protocol was implemented where the modems alternated transmissions and continually cycled through WHOI data rates 0,1,4, and 5 (Table I). Rates 2 and 3 have equivalent packet sizes as rates 1 and 4, but are antiquated and no longer recommended for use [2]. The success or failure of each frame was recorded along with timestamp and AUV pose. The trial held most variables constant in a given day of in-water testing; the AUV was set to traverse a single back-and-forth path in order to improve sample density. In one day, a dense array of frame receipt data was collected for a 1 km path as shown in Fig. 1. This dataset is used to develop a simulation environment with modem models that have realistic frame transmission characteristics.

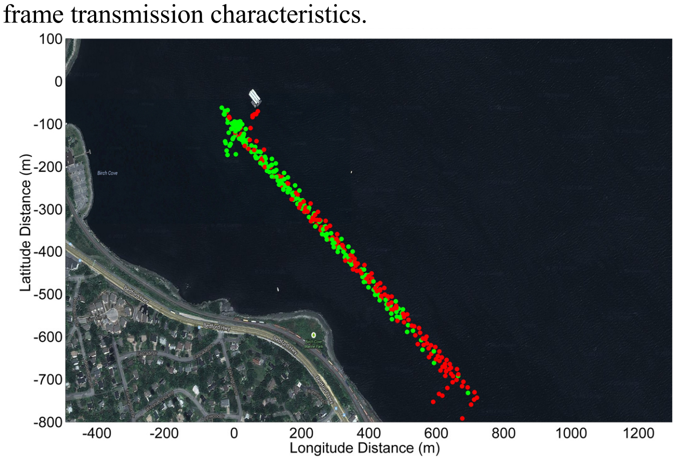

Fig. 1. Satellite view of data rate characterization trials. Green dots represent AUV position at time of successful transmissions, and red dots at time of failed transmissions. White rectangle is ACB on which the deck modem was installed.

III. SIMULATOR DEVELOPMENT

A simulation environment was required to compare the performance of adaptive communications algorithms while minimizing the need for expensive hardware and field trials. The key requirements of the simulator include:

1. multi-vehicle kinematics and path following;
2. conditions representative of the bathymetric and acoustic properties of Bedford Basin;
3. integration with Acoustic Toolbox ray tracing tools;
4. representative and data rate dependent success and failure of the WHOI micromodem packets, and
5. efficient batch computation.

A variety of underwater vehicle simulators are available, including one integrated into the MOOS-IVP autonomy software. However, it was more efficient to build a custom simulator than to modify an existing one to meet all five requirements. The simulator was developed using MATLAB's parallel processing library for ease of coding and quick multi-core batch processing. Fig. 2 details the simulator layout.

The environment and the multiple vehicles interact throughout a collaborative mission. The modem controller is the test seat for adaptive algorithms. At any time that the modem controller directs a vehicle to transmit a packet, the environment is sliced to provide a 2D bottom profile section between source and receiver vehicles. This is input to the BELLHOP ray tracing and Kraken normal modes tools [8] which provide a physics-based transmission loss (TL) calculator. As shown in Fig. 3, in a shallow water environment the TL at any location is heavily dependent on bottom profile, which leads to both multi-path and dead zones.

The Bedford Basin bottom profile, where the modem was deployed above, was modeled using depths from a historic bathymetric survey and a bottom composition of deep, soft mud. This bottom type was modeled with density $\rho = 1.6\ g/cm^3$, speed of sound $c_p = 1490\ m/s$, and bottom

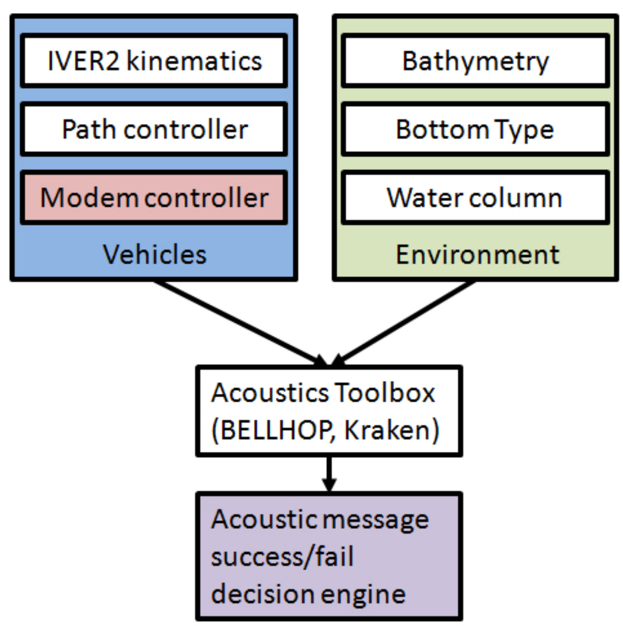

Fig. 2. Block diagram of simulation environment. All blocks except the Acoustics Toolbox were developed by the author.

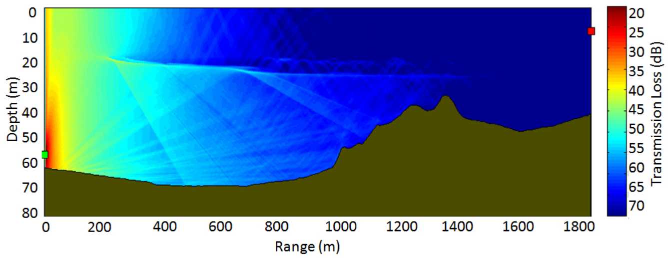

Fig. 3. Example acoustic transmission loss profile for a vehicle-vehicle WHOI micromodem transmission in the simulation environment. The green square represents the source vehicle and the red square the destionation vehicle.

attenuation, $\alpha_p = 1.0\ dB/\lambda$ [9]. The sound speed profile (SSP) was taken from an October 2013 measurement (Fig. 6).

The key innovation in the simulator itself is the decision block (purple, Fig. 2) that governs whether the WHOI micromodem packets are received. This block uses a probabilistic model to relate simulated TL to likelihood of packet success, *P(s),* based on data rate. To generate the TL vs *P(s)* for each data rate, the October sea trial was recreated in the simulated environment. A simulated transmission was performed at each location and time stamp where an actual transmission was performed in the field trial. For each of the four WHOI micromodem data dates, the TL calculated in the simulations was regressed against the packet success in the sea trial (Fig. 4). This regression is used by the decision block to determine the likelihood of success for any given condition. This is less complex than a full simulation of the modem's bit decoding process.

IV. MISSION FACTOR INFLUENCE

Each adaptive acoustic control algorithm is tested against an identical set of simulated scenarios. A shallow water NMCM mission has a large number of factors that may influence acoustic performance. In order to reduce scope, the influence of four of the most significant was quantified to determine which had the greatest impact on acoustic performance. The influence of each factor was tested in a simple, simulated two vehicle mission by calculating the impact of a dichotomy of conditions within each factor: *e.g.* acoustic performance with and without added ambient noise. The impact on acoustic performance was assessed in terms of bandwidth and frequency of successful communications.

A. Mission Path Size

A typical small lawnmower mission in the Bedford Basin is 500m × 500m in size, and the largest possible is approximately 2,000m × 2,000m. Fig. 5 details the two missions compared.

B. Ambient Noise

Ambient noise at the October sea trial is taken into account in the simulator. However, additional noise may be generated through environmental (rain, aquatic life, waves) or anthropogenic (ships, sonar) sources. Ambient noise levels of $0dB$ and $6dB$ were compared; $6dB$ is an estimate for high typical noises in a populated shallow water port.

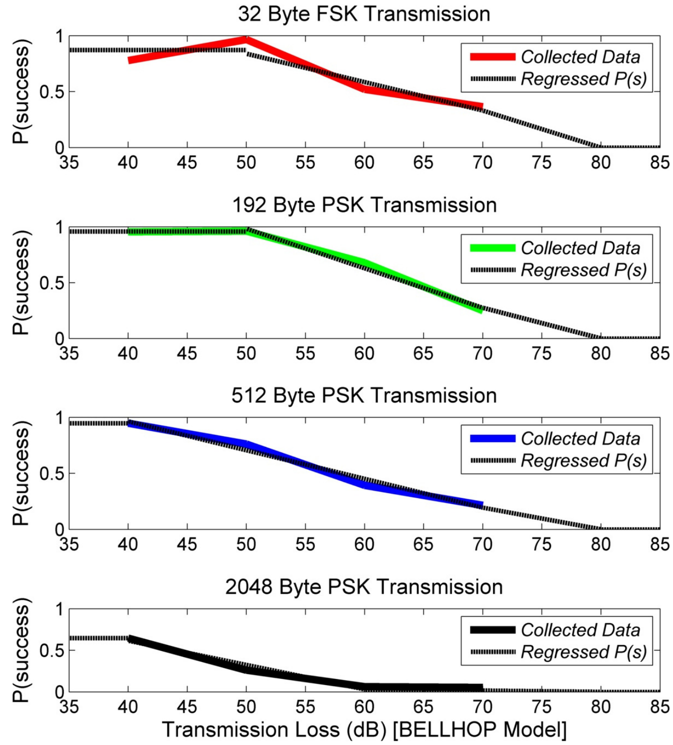

Fig. 4. Comparison of WHOI micromodem probability of frame success versus TL as a function of data rate. Black overlaid lines are the regressed values used in the simulator's packet success decision block .

C. Sound Speed Profile

The SSP varies throughout the year and also after transient weather events such as precipitation. October (summer profile) and May (winter profile) SSPs were compared and are shown in Fig. 6.

D. Vehicle Type

During the October trial, both the IVER2 and deck modem had identical WHOI micromodems and transducers. However, they had different transducer mounts, geometry, and local noise sources. The major performance difference was a tendency for the deck modem to more frequently drop part of a multi-frame packet than the IVER2. As seen in TABLE II, this was seen at

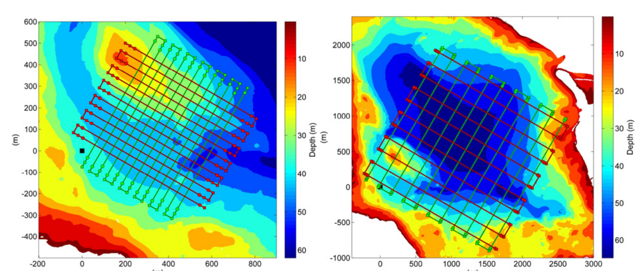

(a) Plan view of small mission path: 500m x 500m square side lawnmower pattern. Red path = AUV1 and green = AUV2.

(a) Plan view of large mission path: 2,000m x 2,000m square side lawnmower pattern. Red path = AUV1 and green = AUV2.

Fig. 5. Mission paths used for simulation of typical small and large shallow-water missions within the Bedford Basin, Halifax, NS, Canada.

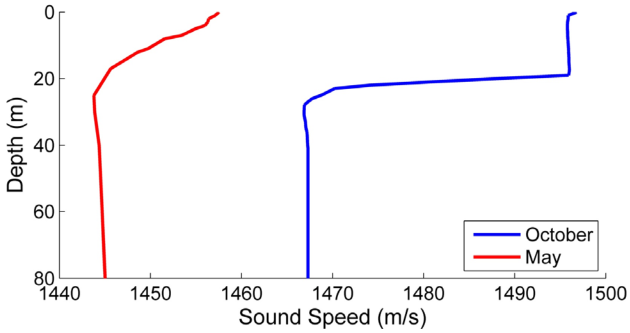

Fig. 6. Seasonal variability in SSP in the Bedford Basin, Halifax, NS, Canada. October profile was collected as part of in water experiments; May profile is taken from [9].

TABLE II. VEHICLE SPECIFIC PARTIAL PACKET LOSS

WHOI Data Rate	% Received Packets Partially Dropped by Barge	% Received Packets Partially Dropped by IVER2
1	38%	8%
4	32%	4%
5	38%	33%

PSK rates 1 and 4 but not rate 5. This may be due to intermittent mechanical noise on the Barge itself.

The influence on overall acoustic performance of these two partial packet reception patterns was compared.

E. Mission Factor Influences

The results of the influence comparison are summarized in Fig. 7. The magnitude of the influence of each factor is simply taken as the difference in performance between the two test cases divided by the performance of the poorer test case. The influence of mission path size and ambient noise are significantly more pronounced than those of the SSP and vehicle type. The SSP had the least influence: it can dramatically influence the path of an acoustic transmission, but not consistently positively or negatively which reduces its long-term impact. The vehicle type also had low impact: the impact of increased partially received frames was not significant compared to the impact of larger missions or higher ambient noise.

1) Simulation Scenarios

The simulation scenarios do not account for differences in SSP or vehicle type due to their low relative influence. This leaves mission size and ambient noise as influences on the four scenarios used for algorithm comparison (TABLE III.

Each adaptive algorithm was run through all four of the above scenarios. To quantify relative algorithm performance, performance criteria were established. Bandwidth, frequency of success, and duty cycle were selected as three criteria demonstrating the most value for high-data NMCM missions. Bandwidth is needed to allow the transfer of information beyond simple status updates. Likewise, frequency of success is important for timely status updates and low duty cycles to reduce on-board power usage, enabling longer missions. Each algorithm's performance against these criterion was normalized to allow summation for a total score (TABLE IV).

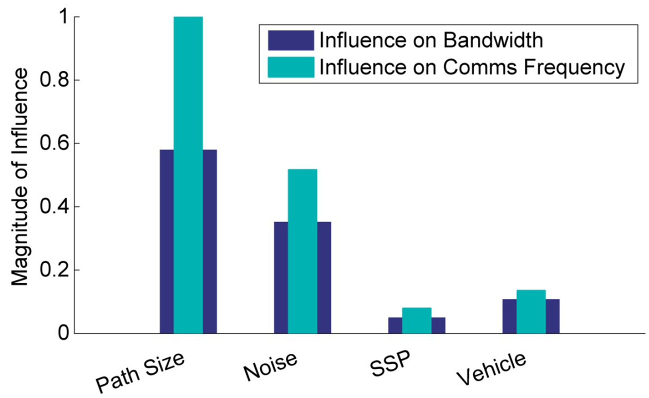

Fig. 7. Influence of four mission factors on acoustic bandwidth and communication frequency. *Path Size* factor represents performance difference between a 500m square side and 2,000m square side lawnmower mission path. *Noise* factor represents performance difference between 0 and 6 dB ambient noise levels. *SSP* represents performance difference between October and May SSPs in Bedford, NS, Canada. *Vehicle* represents difference between the WHOI WH-BT-1 transducer mounted on the IVER2 AUV and mounted on the WHOI towfish statically deployed from a barge.

TABLE III. SIMULATION SCENARIOS

Simulation Scenario	Mission Path	Ambient Noise Level
1	500m x 500m square lawnmower	0dB
2	500m x 500m square lawnmower	6dB
3	2,000m x 2,000m square lawnmower	0dB
4	2,000m x 2,000m square lawnmower	6dB

TABLE IV. ALGORITHM PERFORMANCE CRITERIA

Criterion	Normalization Scoring	Value (%)
Bandwidth (B/s)	Ratio of bandwidth achieved in a scenario versus ceiling. Ceiling is defined as rate 1 transmissions sent every 10 seconds with 100% success (19.2 B/s)	50%
% Duty Cycle	Ratio of transmission opportunities taken to those available.	30%
Frequency of Success	Score of one for any period between updates less than threshold, and half score for each doubling of period past threshold. Threshold determined as 60s for missions where inter-vehicle distance averages less than 500m. For greater inter-vehicle distances, threshold increases by 60s for each additional 500m.	20%

V. ADAPTIVE TRANSMISSION ALGORITHM

Adaptive AUV communication behaviors are an area of active research. Scheider integrates BELLHOP with MOOS-IVP to perform on-line ray tracing and plan the best path for acoustic connectivity with a static source [4]. Chen and Pompili optimize multi-hop packet path planning [5]. However, current work does not well translate to generic missions due to the hardware or mission requirements of the algorithms. For example, rapid deployment with or without prior environmental information may be required in a NMCM mission: adaptive algorithms cannot depend on a priori knowledge of the acoustic environment. The AUV path is completely constrained by the survey requirements of the mission: the path may not be adapted for acoustic optimization. NMCM AUV sensor payloads are focused on sonar and may not incorporate salinity and temperature sensors: acoustic adaptivity cannot depend on the availability of real-time SSPs. Finally, vehicle paths may be fixed or dynamically updated: acoustic optimization may be able to use pre-determined plans but also must be able to estimate the position of collaborating vehicles dynamically if necessary.

These constraints limit the adaptive communications algorithm to controlling only the modem, not the vehicle path. Additionally, not enough sensor information is assured to attempt to directly characterize the acoustics of each transmission. Rather, it was decided to perform a 'forgetful' characterization of the overall performance of the environment as a function of micromodem data rate and range. The adaptivity algorithm is broken into three modules, with the first two feeding information to the third which performs the decision making engine.

1. Position Estimator: estimates collaborating vehicles' position with status updates and, if available, mission plans.
2. Data Transmission Performance Tracker: provides cheaper, more reliable success tracking than the modem's ACK bit
3. Rate Selector: decides whether to attempt a transmit and at which WHOI data rate.

A. Position Estimator

The position estimator is fed the self-reported position and next waypoint of collaborating vehicles each time a status update is successfully received. Between status updates, the estimator uses kinematics to predict the collaborator trajectory between current and next waypoint. A key influence on performance is the mission type: pre-planned or dynamic.

If a vehicle has a priori knowledge of a collaborator's pre-planned mission, then it is able to track it even through long communication droughts by running a kinematics-based waypoint shadow simulation. "Next waypoint" transmissions need only be a one-byte numerical waypoint identifier corresponding to the coordinates of a pre-planned mission point. With a dynamic mission type, performance is degraded but still viable. "Next waypoint" transmissions are full latitude and longitude coordinates which cost 7 bytes overhead. This performance is on par with pre-planned missions if constant contact is maintained, but if information regarding a waypoint is lost the estimator assumes the vehicle stops. This leads to error but is superior to the straight-line assumption which leads to runaway estimations.

B. Data Transmission Performance Tracker

Transmission data success tracking is required in any collaborative AUV application where future actions depend on the success or failure of transmitted messages. Such tracking is not required in basic scenarios: for example, a mission where AUVs simply send periodic status updates to each other [10]. Future actions to send additional status updates are unaffected by whether a status update is received. Short command sequences between heterogenous assets using a common language such as the WHOI Compact Control Language (CCL) [10] are suited to using the WHOI micromodem acknowledgement (ACK) bit. If a command is not received by a hardware asset, another is sent until one is successful.

Similar to command scenarios, data transfer applications such as collaborative SLAM require data transmission performance tracking to ensure complete transfer of critical data and to eliminate expensive redundant transmissions. ACK performs well, but is expensive since it increases cycle time.

The minimum cycle time for a 32 byte rate 0 FSK (frequency shift keying) message is about six seconds [11] [12]. However, this was applied to small mission sizes (200m path length); larger mission sizes require longer cycle time to account for acoustic travel time. 10s cycle time is used for rate 0 and 1 messages [13]. Rate 5 PSK (phase shift keying) messages take even longer due to the slow serial transfers to and from the modem which are theoretically 4.9s [2]. In practice 8s was measured on the IVER2 modem. [14] uses 15 seconds for rate 5. The cycle times for this work were assumed at 10s for rates 0,1,4, and 15s for rate 5.

An ACK bit requires minimal time to generate; the cycle time allocated to it is for the acoustic travel time. The large simulated mission in Fig. 5 has maximum inter-vehicle ranges of 2800m, which is slightly less than 2.0 s of acoustic travel time. Therefore, a 2.0 s cycle time allocation for the ACK bit was assumed for cost comparisons. The bandwidth cost c of using the ACK bit can be calculated by comparing the data transferred, d, to the cycle time, t:

$$\boldsymbol{c} = \frac{\boldsymbol{d}}{\boldsymbol{t}_{\boldsymbol{No\ ACK}}} - \frac{\boldsymbol{d}}{\boldsymbol{t}_{\boldsymbol{ACK}}}. \tag{1}$$

This impact is noted at each micromodem data rate (Fig. 10). Note, this assumes perfect reception of data and ACK packets.

Data transmission performance tracking has the potential to significantly reduce bandwidth costs. [13] implements a cheap system for position estimation sharing, but is limited to synchronizing a small number of repeatedly updated data values. For tracking of arbitrary data, as required for collaborative SLAM, sonar image snippet transfers, or other data intensive application, a more generic tracker is required.

A modular, decentralized software data tracking system was developed to reduce the bandwidth cost of data tracking. The system has two components. First, a database is implemented on each vehicle to track each data frame the vehicle transmitted and whether it was successfully received by the intended recipient(s). Second, tracking headers are included with each transmission to notify collaborators when the vehicle successfully receives packets. When a vehicle (designated AUV1) first sends a packet, the frame contents are added to the tracking database and their received status is set as *unknown.* AUV1 then parses the tracking headers of messages it receives from collaborators. Once it receives confirmation that its previous transmission failed or was received, the received status of those database frame entries is accordingly updated. Once AUV1's collaborators are aware that AUV1 has received feedback on a packet, that feedback is removed from the tracking headers the collaborators transmit.

A key requirement of the data tracking system is minimal data overhead, even in poor acoustic conditions with high packet losses. This is accomplished by designing the tracking headers to explicitly report successfully received packets, but only implicitly report unreceived packets. The tracking headers report how many communication cycles ago each successful packet was received. Implicitly, any packet sent on a communication cycle not reported is assumed failed. This method links tracking header build-up to the unlikely scenario that one collaborator consistently fails to receive packets but succeeds in sending them, rather than to the likely scenario of mutual frequent losses or long blackouts (Fig. 8).

Each queue entry in the *Tracking Header* represents *cycles_ago* using an $\epsilon(0,63)$ integer (7 bit cost when DCCL encoded [7]). Each entry represents *frame_success* using a $\epsilon(0,7)$ integer (4 bit cost in DCCL) for WHOI micromodem data rates 0, 1, and 4 and an $\epsilon(0,255)$ integer (9 bit cost in DCCL) for WHOI micromodem data rate 5. The total size of each queue entry for WHOI modem rates 0-4 is 11 bits, while for rate 5 the cost increases to 16 bits. The mean bandwidth cost of the software data tracker is calculated as follows:

$$\frac{\boldsymbol{queue\ element\ size\ (B) x\ mean\ queue\ length}}{\boldsymbol{cycle\ time\ (s)}} \qquad (2)$$

Mean and maximum tracking header queue lengths for all simulation scenarios are detailed in Fig. 9. The worst-case cost (scenario 4 with a 1.682 mean queue length) is used to generate the software tracking bandwidth cost (Fig. 10). Performance between the software and ACK bit tracking is comparable at data rate 0, but for higher bandwidth PSK data rates the cost of software tracking remains nearly constant while the cost of the hardware ACK bit scales linearly with bandwidth. The system is 100% reliable within the constraint that no tracking header

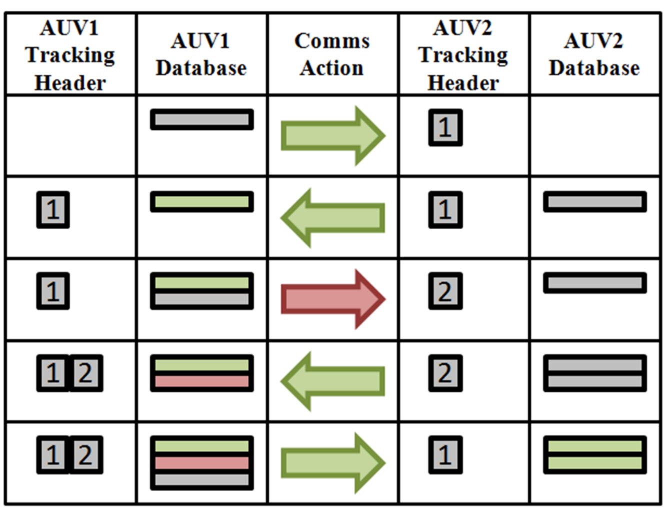

Fig. 8. Snapshot of data tracking system. Each row represents the state of two collaborating AUVs before one transmits and after the other receives. Each arrow under *Comms Action* represents a transmission, with green arrows successful and red failed. Each block under *Database* represents the host AUV's record of one frame it sent, with green representing successful receipt, red failed, and grey unknown. Each block under *Tracking Header* represents one element in the tracking header queue sent by the host AUV, with the number inside representing how many cycles ago the tracked message was received.

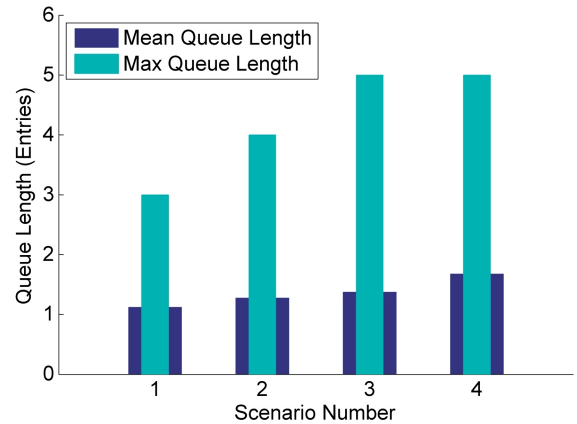

Fig. 9. Tracking header queue length vs simulation scenario. Each queue entry costs 1.625 Bytes for WHOI micromodem rates 0,1,4 while the cost increases to 2.0 Bytes for rate 5.

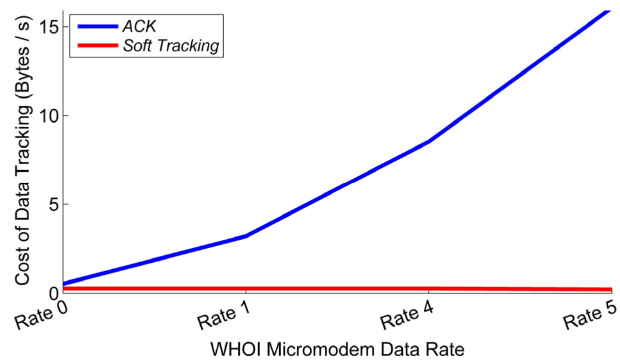

Fig. 10. Impact of data tracking methods on bandwidth. The impact of soft tracking is due to overhead data contained within each packet, while impact of ACK tracking is due to increased cycle times.

queue entries are allowed to age past the upper limit set on the *cycles_ago* variable. *Cycles_ago* was set to a maximum of 63 for the trials: any tracking header not received within 63 cycles is lost and the delivery status of the corresponding packet unknown. This maximum could be increased arbitrarily at the cost of one extra bit in each queue entry each time it doubles.

C. Rate Selector

The rate selector is central to the design of an adaptive communications control algorithm for collaborative work using the WHOI micromodem. When a vehicle reaches the transmit phase of the communication cycle, the rate selector decides whether or not to transmit and, if yes, which data rate should be used. The acoustic environment is both time and geographically variable: to make good decisions, the rate selector must estimate the goodness of the acoustic channel between source and destination vehicles at each moment of transmission. The literature mainly focuses on high level adaptive inter-AUV communication that uses physics-based models to quantitatively estimate the actual acoustic signal loss at the receiver location, either with on-line ray tracing [4] or simple approximations such as the Urick model [5]. [2]'s on-line ray tracing shows promise for applications in depths as shallow as 110m, but it relies on knowledge of the current SSP and assumes a flat bottom. These parameters are not necessarily unavailable for an NMCM mission. [3]'s model approximation is generic in that it does not take environmental and acoustic geometry into consideration. Neither method accounts for ambient noise sources that vary.

The constraints placed by NMCM on AUV environmental knowledge reduces the practicality of a real-time characterization of TL using an on-line physical model of the environment. This led the rate selector design to move from an attempt at acoustic transmission modeling to a forgetful characterization of the current state of the most influential environmental factors. Of the four factors in Fig. 7, mission size and ambient noise have high impact on mean communications performance while that of vehicle type and SSP is low. No characterization of SSP was attempted. Vehicle type also had a low influence, but its characterization is not practically discreet from a vehicle-specific characterization of ambient noise. Therefore, on-line acoustic condition characterization is focused on position and vehicle-specific ambient noise.

An adaptive distance binning model is implemented. The position estimator on-board each vehicle maintains a current estimate of the positions of all collaborating vehicles. Two arrays of distance bins corresponding to each transmission at each WHOI micromodem data rate and also no transmission are maintained in parallel. One array of bins represents a conservative, high-reliability mode for status updates and the other a high-bandwidth mode for data transfer. Data bins are used by default unless performance is degraded beyond a threshold, at which point status bins are used until connectivity is regained. At each decision point, the rate selector chooses the transmission type corresponding to the bin that encompasses the current distance to the intended recipient(s). The upper and lower bin boundaries are pre-set at the mission start and adapted on-line throughout the mission. This on-line adaptation is controlled by setting desired success ratios for transmissions at each data rate. This is shown in Fig. 11 where uppercase symbols represent pre-set parameters and lowercase represent calculated variables:

Δ = *status transmission threshold* (controls # sequential failed transmission attempts before moving to the low-rate bins)
β = *WHOI micromodem data rate* (selected for transmission)
γ = *status bin* or *data bin* (current distance between the source and receiving AUV)
$p(s)$ = current estimation of *probability of success* for β.
Γ = *memory length* (controls # previous transmissions incorporated into the estimate of current *p(s)* for β)
Π = *target success ratios* (represents desired success ratio for each micromodem data rate Π_β = desired success ratio for β)
Υ = *target success tolerance* (values of $p(s)$ within Υ of Π_β are considered to be at the target ratio)
Θ = *bin increment value* (if $p(s)$ is not within Υ of Π_β, γ is increased Θ in a direction to encourage $p(s)$ to approach Π_β)

The adaptive engine is driven by the need for $p(s)$ of each data rate to approach the target success ratios Π. This method is robust to environmental change. For e.g. a poor acoustic environment will initially yield a $p(s)$ below the desired success ratio Π_β. In this case, the distance of bin γ will be decreased, meaning subsequent communications at that rate will take place closer to the recipient, increasing $p(s)$. The reverse occurs in

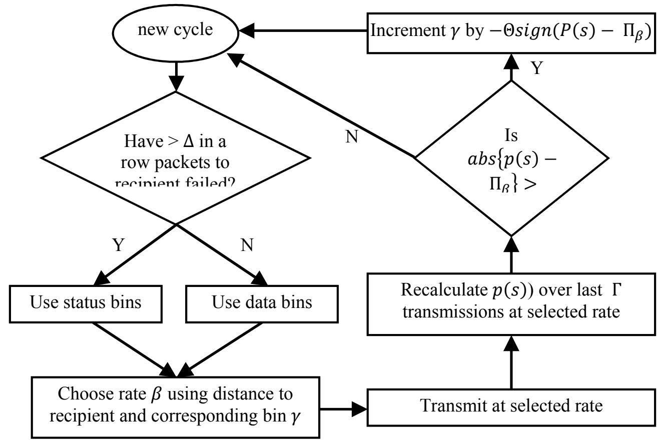

Fig. 11. Rate selector program flow. Adaptation comes from learning which distance bins provide the desired *p(s)* in the current environment, rather than to model the complex shallow water acoustic environment.

an unusually good environment. It is desirable for the rate selector to target success ratios directly as $p(s|\beta)$ can be directly translated to high-level mission communication outcomes such as desired frequency of status updates, duty cycle power usage, etc.

The bins are optimized on-line; their start values do not significantly impact performance due to their continual revision. However, the pre-set parameters do significantly impact performance. Hundreds of parameter combinations were test-run on all four simulation scenarios to determine the most optimal values (TABLE V)

The performance of the optimal parameters are compared to control communication schemes in the following sections. Three controls are used. First, continual use of rate 0; this is one of the most commonly used WHOI micromodem control schemes [13]. Second, continual use of rate 1; this is proposed by Fallon [13] as a bandwidth improvement over rate 0. Third, alternating use of rate 0 and rate 5: this is used by Schneider

TABLE V. RATE SELECTOR PARAMETER TUNING

Parameter	Values Tested in Simulation	Optimal Value
Target Success Ratios $[\Pi_5;\ \Pi_4;\ \Pi_1;\ \Pi_0]$	[0-0.5 ; 0.2-0.7 ; 0.3-0.8 ; 0[1]]	[0[2] 0.3 0.4 0]
Memory Length Γ	10-20 transmissions	10
Target Success Tolerance Υ	0.05[3]	0.05
Bin Increment Value Θ	5-20 meters	5
Status Transmission Threshold Δ	2-4	3

[1]After performing transmission loss versus *p(s)* calculations as shown in Fig. 4, it was found that the *p(s)* of rate 0 communications closely matched the *p(s)* of rate 1 communications. With a factor of six improvement in bandwidth, rate 1 was always preferred over rate 0 in the rate selector design.

[2] If cycle time is held constant, having nonzero target success ratios for data rate 5 proves superior to a zero value success ratio. However, the longer serial communication time required for rate 5 forces the network to jump from a 10s to 15s cycle time due to TDMA constraints. Taking this into consideration, 10s cycle times that do not use rate 5 prove superior.

[3] Target success tolerance was not varied during simulations due to computing budget constraints.

and Schmidt as a compromise between high bandwidth and reliability [3]. For reference, also included are a set of parameters that are optimal in the event rate 5 is implemented; however, the longer cycle time inherent with rate 5 reduces the effectiveness of this solution.

1) *Bandwidth*

Mean successful data throughput was compared (Fig. 12). The adaptive algorithm without rate 5 proves superior to all control methods, even the intermittent use of high-bandwidth rate 5. Important to note is how it uses high bandwidth rates to capitalize on the good acoustic conditions of the a small, low-noise scenario 1 while retaining connectivity using lower rates in the large, noisy scenario 4.

2) *Status Update Period*

Mean period between successful transmissions was examined (not shown). The adaptive algorithm without rate 5 proves superior to alternating of rates 0 and 5, but inferior to continual communications at either rate 0 or 1. While not ideal, this is acceptable because of performance gains in the other two categories. Adaptive rate control does not improve the underlying goodness of the acoustic channel; it merely allows the operator to achieve a desired combination of performance in the mutually detrimental categories of bandwidth, update frequency, and power usage. This particular optimization prioritized bandwidth and low power usage while ensuring reasonable status update frequency.

3) *Power Usage*

Both adaptive algorithms are comparable to the continual duty cycle control methods in the small mission size, but drop to less than fifty percent for the larger mission (not shown).

VI. Conclusions

An adaptive framework has been presented that provides AUV operators a method to optimize acoustic modem performance in collaborative AUV missions regardless of constraints imposed by areas such as NMCM. The key contributions are (1) a robust software data tracking transmission performance system that is more reliable than the ACK hardware bit while costing significantly less bandwidth and (2) an adaptive data rate decision engine that yields improved bandwidth and reduced duty cycles compared to traditional, non-adaptive methods.

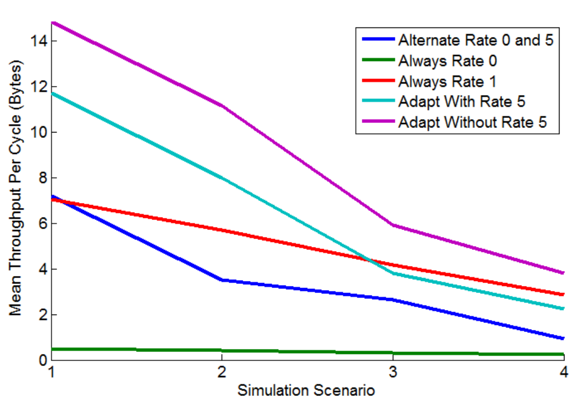

Fig. 12. Adaptive algorithm data throughput performance comparison. The adaptivity without rate 5 significantly outperformed all others.

The framework has been applied to a variety of operating environments and yielded promising results in simulated collaborative AUV missions. Currently the framework is in the final stage of porting from MATLAB simulation and integrated with MOOS-IVP enabled IVER3 AUVs. Its effect on bandwidth, connectivity, and duty cycle will be evaluated in a variety of conditions and environments to determine its ability to improve in-water communications for collaborative missions.

Acknowledgements

This work was supported in part by ONR Global grant N62909-12-1-7051.

References

[1] M. Seto, L. Paull and S. Saeedi, "Introduction to Autonomy for Marine Robots," in *Marine Robot Autonomy*, M. Seto, Ed., Springer, 2012, pp. 1-40.

[2] L. Freitag, "Micro-Modem Software Interface Guide," Woods Hole Oceanographic Institution, Woods Hole, 2013.

[3] T. Schneider and H. Schmidt, "Unified Command and Control for Heterogeneous Marine Sensing Networks," *Journal of Field Robotics,* vol. 27, no. 6, pp. 876-889, 2010.

[4] T. Schneider and H. Schmidt, "Model-Based Adaptive Behavior Framework for Optimal Acoustic Communication and Sensing by Marine Robots," *Oceanic Engineering, IEEE Journal of ,* vol. 38, no. 3, pp. 522-533, 2013.

[5] B. Chen, P. Hickey and D. Pompili, "Trajectory-Aware Communication Solution for Underwater Gliders Using WHOI Micro-Modems," in *Sensor Mesh and Ad Hoc Communications and Networks (SECON)*, 2010.

[6] P. Newman, "MOOS - Mission Orientated Operating Suite," Boston, USA.

[7] T. Schneider and H. Schmidt, "The Dynamic Compact Control Language: A Compact Marshalling Scheme for Acoustic Communications," in *OCEANS 2010 IEEE* , Sydney, 2010.

[8] M. Porter, "Bellhop Code," 2014. [Online]. Available: http://oalib.hlsresearch.com/Rays/index.html. [Accessed September 2014].

[9] D. Nams, "Online Bandwidth Adaptation and Data Tracking of Underwater Acoustic Transmissions to Optimize Communications for Collaborative AUV Missions," MASc Thesis, Dept. of Mech. Eng, Dalhousie, Halifax, NS, 2014.

[10] R. F. L. G. M. Stokey, "A Compact Control Language for AUV Acoustic Communication," in *OCEANS 2005*, 2005.

[11] N. Hallin, H. Taheri, J. Horn, M. ORourke and D. Edwards, "Architecture and applications of Language-Centered Intelligence for unmanned underwater vehicles," in *Systems, Man, and Cybernetics (SMC), 2011 IEEE International Conference on*, 2011.

[12] T. Bean, G. Beidler, J. Canning, D. Odell, R. Wall, M. O'Rourke, M. Anderson and D. Edwards, "Language and Logic to Enable Collaborative Behavior among Multiple Autonomous Underwater Vehicles," *International Journal of Intelligent Control and Systems,* vol. 13, no. 1, pp. 67-80, March 2008.

[13] M. F. Fallon, G. Papadopoulos and J. J. Leonard, "A measurement distribution framework for cooperative navigation using multiple AUVs," in *Robotics and Automation (ICRA), 2010 IEEE International Conference on*, 2010.

[14] F. Maurelli, P. Patron, J. Cartwright, J. Sawas, Y. Petillot and D. Lane, "Integrated MCM missions using heterogeneous fleets of AUVs," in *OCEANS, 2012*, 2012.